Heisenberg-scaled magnetometer with dipolar spin-1 condensates

Haijun Xing,[1] Anbang Wang,[1] Qing-Shou Tan,[1] Wenxian Zhang,[2] and Su Yi[1]

[1]*Key Laboratory of Theoretical Physics, Institute of Theoretical Physics, Chinese Academy of Sciences, P.O. Box 2735, Beijing 100190, China*
[2]*School of Physics and Technology, Wuhan University, Wuhan, Hubei 430072, China*

We propose a scheme to realize a Heisenberg-scaled magnetometer using dipolar spin-1 condensates. The input state of magnetometer is prepared by slowly sweeping a transverse magnetic field to zero, which yields a highly entangled spin state of N atoms. We show that this process is protected by a parity symmetry such that the state preparation time is within the reach of the current experiment. We also propose a parity measurement with a Stern-Gerlach apparatus which is shown to approach the optimal measurement in the large atom number limit. Finally, we show that the phase estimation sensitivity of the proposed scheme roughly follows the Heisenberg scaling.

I. INTRODUCTION

The detection of ultralow magnetic fields plays an important role in diverse areas of research ranging from the fundamental physics [1–4] to a wide range of practical applications in sciences and technologies [5–11]. Following the development of quantum metrology [12–14], it is realized that utilizing quantum resources such as entanglement [15–18] can improve the precision of parameter estimation from the shot-noise limit (standard quantum limit) to the Heisenberg limit [19–21]. In the context of quantum metrology, state preparation (together with parametrization) often represents an important step for precision measurement as it determines the amount of the quantum Fisher information (FI) that can be extracted from a quantum state. Through the Cramér-Rao inequality, the FI then set the lower bound for the uncertainty of the parameter estimation such that a parameter can be estimated with higher precision if the state has a larger FI. It has been shown that states such as NOON states [22–24], spin squeezed states [25,26], twin Fock states [20,27–29], and entangled coherent states [30–32] are candidates for achieving the beyond shot-noise-limit measurements. In recent years, quantum-enhanced magnetometers are proposed in various systems [33–47].

In this work, we propose a magnetometer based on the adiabatic protocol that produces the maximally entangled spin states using dipolar spin-1 condensates [48]. Under the single-mode approximation (SMA), we discover a parity symmetry which divides the Hilbert space of a spin-1 condensate of N atoms into even- and odd-parity subspaces; in particular, the maximally entangled spin state (the input state of our magnetometer) belongs to the even-parity subspace. We show that, in the state preparation stage, the Hamiltonian of the system conserves the parity symmetry, which significantly loosen the adiabatic condition required for generating the maximally entangled spin state. As a result, the time required for state preparation is within the reach of current experiments. We also propose a parity measurement scheme using a Stern-Gerlach apparatus, which approaches the optimal measurement in the large N limit. Finally, we show that the phase estimation sensitivity roughly scales with $1/N$, indicating that the proposed magnetometer is at the level of the Heisenberg limit. We notice that spinor-condensate-based magnetometers are experimentally demonstrated recently [49,50].

This paper is organized as follows. In Sec. II, we introduce the model Hamiltonian and the scheme for the Heisenberg-scaled magnetometer. In the context of quantum metrology, we present a detailed analysis about each stage of the magnetometer in Sec. III. The numerical simulations about the performance of the magnetometer are presented in Sec. IV. Finally, we conclude in Sec. V.

II. MODEL

We consider N Bose condensed spin $F = 1$ atoms confined in an axially symmetric potential whose symmetry axis is chosen as the quantization axis, $\hat{\mathbf{z}}$, of the system. Under the SMA, all three spin components $\alpha = 0, \pm 1$ share a common spatial mode $\psi(\mathbf{r})$. The Hamiltonian for the condensate subjected to an external magnetic field $\mathbf{B}'$ takes the form [51]

$$H' = (c_2' - c_d')\hat{\mathbf{S}}^2 + 3c_d'(\hat{S}_z^2 + \hat{n}_0) - g_F\mu_B\mathbf{B}' \cdot \hat{\mathbf{S}}, \quad (1)$$

where $\hat{\mathbf{S}} = \sum_{\alpha\beta} \hat{a}_\alpha^\dagger \mathbf{F}_{\alpha\beta} \hat{a}_\beta$ is the many-body total spin operator with $\hat{a}_\alpha$ being the annihilation operator of the αth spin state and $\mathbf{F}$ the angular momentum operator, $\hat{S}_z$ is the z component of $\hat{\mathbf{S}}$, and $\hat{n}_0 = \hat{a}_0^\dagger \hat{a}_0$ is the number operator of the $\alpha = 0$ spin component.

In Hamiltonian Eq. (1), the spin-exchange interaction strength is

$$c_2' = \frac{c_2}{2} \int d\mathbf{r} |\psi(\mathbf{r})|^4,$$

where $c_2 = 4\pi\hbar^2(a_2 - a_0)/(3M)$ with M being the mass of the atom and a_f ($f = 0,2$) the s-wave scattering length for two spin-1 atoms in the combined symmetric channel of total spin f. The dipolar interaction is characterized by

$$c_d' = \frac{c_d}{4} \int d\mathbf{r}\, d\mathbf{r}' |\psi(\mathbf{r})|^2 |\psi(\mathbf{r}')|^2 \frac{1 - 3\cos^2\theta_{\mathbf{r}-\mathbf{r}'}}{|\mathbf{r} - \mathbf{r}'|^3},$$

where $\theta_{\mathbf{r}-\mathbf{r}'}$ is the polar angle of the vector $(\mathbf{r} - \mathbf{r}')$ and $c_d = \mu_0\mu_B^2 g_F^2/(4\pi)$ is the strength of the magnetic dipole-dipole interaction with μ_0 being the vacuum magnetic permeability, μ_B the Bohr magneton, and g_F the Landé g factor.

Although the sign of c_2' is determined by that of c_2, the sign of c_d' depends on the geometry of the trapping potential: $c_d' < 0$ (> 0) for elongated (prolate) trap. In this
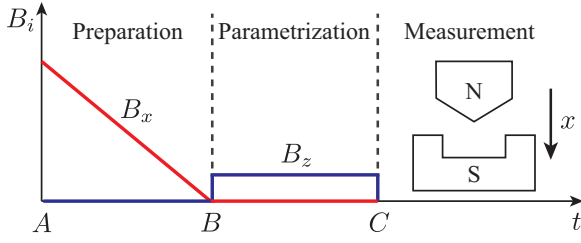
FIG. 1. Schematic plot of the scheme.

work, we assume that the spin-exchange collisional interaction is ferromagnetic ($c_2 < 0$) and the trapping potential is highly elongated ($c_d' < 0$). Under these conditions, the condensate falls into the ferromagnetic phase and the SMA holds even when $c_d > |c_2|$ in the absence of the external magnetic field [51,52]. In particular, in Refs. [53,54], it was shown that the SMA is valid for describing the spin dynamics of spin-1 Rb condensates. We therefore expect that the adoption of the SMA should not affect our conclusions.

For convenience, we rescale Eq. (1) using the energy unit $|c_2'|$ (the corresponding unit for time is then $\hbar/|c_2'|$), which yields the dimensionless Hamiltonian [48]

$$H = H_0 + H_1, \tag{2}$$

$$H_0 = (-1 - c)\hat{\mathbf{S}}^2 + 3c\hat{S}_z^2 - \mathbf{B} \cdot \hat{\mathbf{S}}, \tag{3}$$

$$H_1 = 3c\hat{n}_0, \tag{4}$$

where $c = c_d'/|c_2'|$ and $\mathbf{B} = g_F \mu_B \mathbf{B}'/|c_2'|$. Although $\hat{n}_0$ does not commute with $\hat{\mathbf{S}}^2$, its contribution is often negligible in the ferromagnetic state. In the absence of external field, the ground states of $H_0, |N, \pm N\rangle_z$, are doubly degenerate, where $|S, m\rangle_z$ denotes the simultaneous eigenstates of $\hat{\mathbf{S}}^2$ and $\hat{S}_z$ with $S = N, N - 2, \ldots \geqslant 0$ and $|m| \leqslant S$ [55].

A particularly attractive feature of this system is that the twofold degeneracy of the ground state can be employed to create the maximally entangled state of N atoms [48]. Specifically, we prepare the condensate under a strong transverse magnetic field, $\mathbf{B} = B_x \hat{\mathbf{x}}$, which polarizes all spins along the x axis. As a result, the wave function of the condensate becomes

$$\left|\Psi_A^{(0)}\right\rangle = |N, N\rangle_x, \tag{5}$$

where $|S, m\rangle_x$ denote the simultaneous eigenstates of $\hat{\mathbf{S}}^2$ and S_x. We then gradually reduce B_x to zero with a constant rate $v_B = dB_x/dt < 0$. For sufficiently small v_B, the wave function of the system evolves into a maximally entangled state [48]

$$\left|\Psi_B^{(0)}\right\rangle = \frac{1}{\sqrt{2}}(|N, N\rangle_z + |N, -N\rangle_z), \tag{6}$$

which can be used as the input state for the magnetometer.

As schematically shown in Fig. 1, we follow the general protocol for parameter estimations to complete the construction of the magnetometer. In the parametrization, we switch on a longitudinal magnetic field $\mathbf{B} = B_z \hat{\mathbf{z}}$ (B_z is the unknown field strength) for a period of time τ. This longitudinal field induces a dynamic phase $\theta = -B_z \tau$ which is the parameter to be estimated. In the measurement stage, we let the condensate pass through a Stern-Gerlach apparatus which is composed
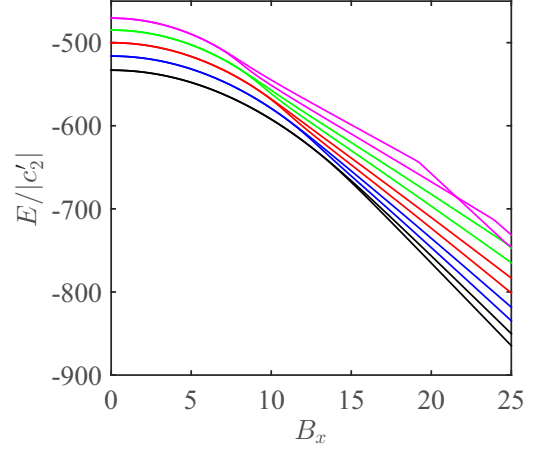

FIG. 2. Transverse field dependence of the lowest 10 energy levels of the Hamiltonian (2) for $N = 20$ and $c = -0.145$. The magnetic field strength B_x is a dimensionless quantity.

of an inhomogeneous magnetic field along the x axis. This allows us to measure $\hat{S}_x$ of the condensate. Finally, we estimate the uncertainty of the whole process. In the next section, we discuss each stage in detail.

III. QUANTUM METROLOGY WITH DIPOLAR SPIN-1 CONDENSATES

In this section, we shall only consider the Hamiltonian H_0 for simplicity. The effects of H_1 will be discussed in the next section. For the Hamiltonian H_0, $\hat{\mathbf{S}}^2$ is conserved. Since the total angular momentum of the initial state, $|\Psi_A^{(0)}\rangle$, is $S = N$, the system can only evolve in the $S = N$ subspace. Therefore, we shall also adopt the shorthand notation $|m\rangle_{x,z}$ for $|N, m\rangle_{x,z}$ in this section.

A. State preparation

To analyze the process of initial state preparation, we plot, in Fig. 2, energy spectrum of the Hamiltonian (3) subjected to a transverse field B_x. At $B_x = 0$, $|S, m\rangle_z$ is the eigenstate of H_0 and the states $|S, \pm m\rangle_z$ ($m \neq 0$) are doubly degenerate. In particular, the ground states in the absence of the external field are $|N, \pm N\rangle_z$. In the large B_x limit, let us focus on the lowest two energy levels. Since the term $-B_x \hat{S}_x$ dominates in H_0, the ground and first excited states are $|N, N\rangle_x$ and $|N, N - 1\rangle_x$, respectively. Treating the spin $\hat{\mathbf{S}}$ classically, it can be easily shown that the system saturates at a critical magnetic field $B_x = -6cN$ such that the spins are completely polarized, while for $B_x < -6cN$ the ground state is doubly degenerate [48]. Although, quantum mechanically, this twofold degeneracy is lifted by quantum tunneling, the energy gap between the ground, $|N, N\rangle_z + |N, -N\rangle_z$, and the first excited, $|N, N\rangle_z - |N, -N\rangle_z$, states is negligibly small for small B_x, which may invalidate the adiabatic condition. Consequently, one would naively expect that the real state obtained at the state preparation stage, $|\Psi_B\rangle$, is an arbitrary superposition of $|N, N\rangle_z$ and $|N, -N\rangle_z$. And even worse, it may also contain the contributions from higher excited states at $B_x = 0$. The numerical simulations however

indicate that the ideal initial state $|\Psi_B^{(0)}\rangle$ is very robust against different sweeping rates v_B [48]. Below, we show that the maximally entangled state $|\Psi_B^{(0)}\rangle$ is partially protected by a *parity symmetry* of the system.

To introduce this parity symmetry, we consider the Fock state basis, $|n_1, n_0, n_{-1}\rangle$, where n_α denotes the occupation number of the αth spin component satisfying the constraint $N = \sum_\alpha n_\alpha$. We then define the *parity operator* $\hat{\mathcal{P}}$ through the equation

$$\hat{\mathcal{P}}|n_1, n_0, n_{-1}\rangle = |n_{-1}, n_0, n_1\rangle. \tag{7}$$

Namely, $\hat{\mathcal{P}}$ exchanges the occupation numbers of the $\alpha = 1$ and -1 spin states. Clearly, $\hat{\mathcal{P}}$ is Hermitian. It can be further shown that

$$\hat{\mathcal{P}}\hat{a}_\alpha = \hat{a}_{-\alpha}\hat{\mathcal{P}}, \tag{8}$$

which leads to

$$[\hat{\mathcal{P}}, \hat{\mathbf{S}}^2] = [\hat{\mathcal{P}}, \hat{S}_z^2] = [\hat{\mathcal{P}}, \hat{S}_x] = [\hat{\mathcal{P}}, \hat{n}_0] = 0. \tag{9}$$

Therefore, in the state preparation stage, both H_0 and H_1 commute with $\hat{\mathcal{P}}$. Furthermore, it can be shown that $\hat{S}_y$ and $\hat{S}_z$ anticommute with $\hat{\mathcal{P}}$, i.e.,

$$\{\hat{\mathcal{P}}, \hat{S}_y\} = \{\hat{\mathcal{P}}, \hat{S}_z\} = 0. \tag{10}$$

In particular, because of $\hat{\mathcal{P}}^2 = 1$, the eigenvalues of $\hat{\mathcal{P}}$ are $\xi = \pm 1$. Thus, based on the eigenvalues of $\hat{\mathcal{P}}$, we may partition the Hilbert space into even- ($\xi = 1$) and odd- ($\xi = -1$) parity subspaces. In fact, as shown in the Appendix III C, the parity operator $\hat{\mathcal{P}}$ can be constructed explicitly as

$$\hat{\mathcal{P}} = \sum_{S,m} |S, m\rangle_{zz}\langle S, -m|. \tag{11}$$

Therefore, the states $|\phi_{S,m}^{(e)}\rangle_z \equiv (|S, m\rangle_z + |S, -m\rangle_z)/\sqrt{2}$ ($m > 0$) and $|\phi_{S,0}^{(e)}\rangle_z = |S, 0\rangle_z$ have even parity, while the parity of the states $|\phi_{S,m}^{(o)}\rangle_z \equiv (|S, m\rangle_z - |S, -m\rangle_z)/\sqrt{2}$ ($m > 0$) is odd. Moreover, because $\hat{\mathcal{P}}$ commutes with $\hat{\mathbf{S}}^2$ and $\hat{S}_x$, the state $|S, m\rangle_x$ has a definite parity. It is shown in the Appendix III C that the parity of $|S, m\rangle_x$ is even (odd) if $N - m$ is even (odd).

Now, since the initial state of the condensate $|\Psi_A^{(0)}\rangle$ has an even parity and the Hamiltonian H_0 commutes with $\hat{\mathcal{P}}$, the final state at $B_x = 0$ must also have an even parity. This constraint significantly loosens the adiabatic condition as it is now determined by the energy gap between the ground and the second excited states, which is finite for all B_x. The above analysis explains why we always obtain the maximally entangled state $|\Psi_B^{(0)}\rangle$ under a sufficiently small constant sweeping rate. We remark that it can be shown that similar parity symmetry can also be found in other systems [56].

Experimentally, it is preferable to have the state preparation time as short as possible. Therefore, it is necessary to consider the sweeping rate beyond the adiabatic condition. When the adiabatic condition is violated, we end up with a general even-parity state

$$|\Psi_B\rangle = \sqrt{p_0}|0\rangle_z + \sum_{m=1}^{N}\sqrt{\frac{p_m}{2}}e^{i\varphi_m}(|m\rangle_z + |-m\rangle_z), \tag{12}$$

where the probability p_m and the phase φ_m can only be obtained numerically for a given sweeping rate.

B. Parametrization

Starting with $|\Psi_B\rangle$, we enter the stage of parametrization by applying a longitudinal magnetic field for a period of time τ. The wave function of the condensate then evolves into

$$|\Psi_C\rangle = \sqrt{p_0}|0\rangle_z + \sum_{m=1}^{N}\sqrt{\frac{p_m}{2}}e^{i\varphi_m}(e^{-im\theta}|m\rangle_z + e^{im\theta}|-m\rangle_z), \tag{13}$$

where we have included the contribution from the $3c\hat{S}_z^2$ term into φ_m. The Fisher information of this state is

$$F = 4\sum_{m=0}^{N} p_m m^2, \tag{14}$$

which determines the lower bound of the variance of the estimator. The maximal Fisher information, $4N^2$, is attained for a maximally entangled state.

It should be noted that, in the state preparation stage, the parity symmetry not only prohibits the transition from the ground state to odd parity subspace, but also guarantees the states $|m\rangle_z$ and $|-m\rangle_z$ in Eq. (13) are equally populated. This property prevents the fast dropping of the Fisher information when the adiabatic condition is violated.

C. Measurement

Now, we turn to consider the measurement. In general, the Fisher information Eq. (14) can only be achieved with the optimal measurement, which is unknown for our system. Here, we propose to measure the observable operator $\hat{\mathcal{O}} = (-1)^{\hat{N}-\hat{S}_x}$, which can be performed using the Stern-Gerlach apparatus depicted in Fig. 1. A close inspection of $\hat{\mathcal{O}}$ indicates that measurement of $\hat{\mathcal{O}}$ is of the parity-measurement-type since (see the Appendix)

$$\hat{\mathcal{O}} = \sum_{S,m}(-1)^{N-m}|S, m\rangle_{xx}\langle S, m| = \hat{\mathcal{P}}. \tag{15}$$

To calculate the mean value of $\hat{\mathcal{O}}$, we rewrite Eq. (13) based on the parities

$$|\Psi_C\rangle = \sqrt{P_e}|\Phi_N^{(e)}\rangle + \sqrt{P_o}|\Phi_N^{(o)}\rangle. \tag{16}$$

Here $P_e = \sum_{m=0}^{N} p_m \cos^2(m\theta)$, $P_o = \sum_{m=1}^{N} p_m \sin^2(m\theta)$, and

$$\left|\Phi_N^{(e)}\right\rangle = \sum_{m=0}^{N} e^{i\varphi_m}\sqrt{\frac{p_m}{P_e}}\cos(m\theta)\left|\phi_{N,m}^{(e)}\right\rangle_z,$$

$$\left|\Phi_N^{(o)}\right\rangle = \sum_{m=1}^{N} e^{i(\varphi_m+3\pi/2)}\sqrt{\frac{p_m}{P_o}}\sin(m\theta)\left|\phi_{N,m}^{(o)}\right\rangle_z. \tag{17}$$

Since, for a reasonable sweeping rate, only those levels with m close to N are populated in Eq. (17) (see the numerical simulations in Sec. IV), it is convenient to introduce the notation, $\ell \equiv N - m$, for the index of the energy levels.

By assuming that $p_{N-\ell} \neq 0$ only when $\ell \leqslant \bar{\ell}$, the quantum mechanics mean value and the variance of $\hat{\mathcal{O}}$ are, respectively,

$$f(\theta) \equiv \langle \hat{\mathcal{O}} \rangle = \sum_{\ell=0}^{\bar{\ell}} p_{N-\ell} \cos\left[2(N-\ell)\theta\right] \qquad (18)$$

and

$$\delta^2 \mathcal{O} = 1 - \left(\sum_{\ell=0}^{\bar{\ell}} p_{N-\ell} \cos\left[2(N-\ell)\theta\right]\right)^2. \qquad (19)$$

D. Parameter estimation

Experimentally, the measurement of $\hat{\mathcal{O}}$ will be repeated for ν times for a given set of parameters, which leads to the outcomes $\xi_1, \xi_2, \ldots, \xi_\nu$. The average value of these measurement results, $\mathcal{O}_{\mathrm{est}} = \nu^{-1} \sum_{i=1}^{\nu} \xi_i$, is the estimator of $\langle \hat{\mathcal{O}} \rangle$. Furthermore, the statistical average of $\mathcal{O}_{\mathrm{est}}$ and its mean-square error are $\langle \mathcal{O}_{\mathrm{est}} \rangle_{\mathrm{av}} = \langle \hat{\mathcal{O}} \rangle$ and $\delta^2 \mathcal{O}_{\mathrm{est}} = \nu^{-1} \delta^2 \mathcal{O}$, respectively. To find the value of θ from these measurements, we need to define its estimator, θ_{est}, which can be most conveniently obtained by inverting Eq. (18). It should be noted that, for f to be invertible, we must have an interval of θ within which f is a monotonic function. Although it is impossible to predict the monotone interval theoretically as $p_{N-\ell}$ are unknown, it can be achieved by experimentally measuring $\hat{\mathcal{O}}$ as a function of τ. From this, we can determine the monotone interval of f in principle. Now, let us formally define the unbiased estimation function of θ as the inverse function of f, i.e.,

$$\theta_{\mathrm{est}} \equiv f^{-1}(\mathcal{O}_{\mathrm{est}}), \qquad (20)$$

whose mean-square error is

$$\begin{aligned}
\delta^2 \theta_{\mathrm{est}} &= \frac{\delta^2 \mathcal{O}}{\nu \left(\partial \langle \hat{\mathcal{O}} \rangle / \partial \theta\right)^2} \\
&= \frac{1 - \left(\sum_\ell p_{N-\ell} \cos[2(N-\ell)\theta]\right)^2}{4\nu \left(\sum_\ell p_{N-\ell}(N-\ell) \sin[2(N-\ell)\theta]\right)^2}.
\end{aligned} \qquad (21)$$

In the limiting case $\bar{\ell} = 0$, we reproduce the well-known Heisenberg limit, $\delta^2 \theta_{\mathrm{est}} = 1/(4\nu N^2)$, which also indicates that θ_{est} is the optimal estimator if a maximally entangled state is prepared.

For the general case, one has to make a further assumption to find how $\delta^2 \theta_{\mathrm{est}}$ scales with N from Eq. (21). Here, we assume that $\bar{\ell}\theta \ll N\theta < \pi/4$, which can always be fulfilled for sufficiently small τ. As a result, to the first oder of $\bar{\ell}\theta$, Eq. (18) becomes approximately

$$\langle \hat{\mathcal{O}} \rangle \approx g(\theta) \equiv \cos(2N\mathcal{L}\theta), \qquad (22)$$

where

$$\mathcal{L} \equiv \sum_{\ell=0}^{\bar{\ell}} p_{N-\ell}\left(1 - \frac{\ell}{N}\right) \leqslant 1 \qquad (23)$$

is the average value of $(1 - \ell/N)$. Equation (22) inspires us to define the estimator of θ as

$$\theta'_{\mathrm{est}} \equiv g^{-1}(\mathcal{O}_{\mathrm{est}}) = \frac{\cos^{-1} \mathcal{O}_{\mathrm{est}}}{2N\mathcal{L}}. \qquad (24)$$

By noting that the variance, Eq. (19), can be approximated as

$$\delta^2 \mathcal{O} \approx 1 - g^2(\theta), \qquad (25)$$

we obtain

$$\begin{aligned}
\delta^2 \theta'_{\mathrm{est}} &= \frac{\delta^2 \mathcal{O}}{\nu [\partial g(\theta)/\partial\theta]^2} \approx \frac{1 - g^2(\theta)}{\nu [\partial g(\theta)/\partial\theta]^2} \\
&= \frac{1}{4\nu N^2 \mathcal{L}^2}.
\end{aligned} \qquad (26)$$

Clearly, to ensure that $\delta^2 \theta'_{\mathrm{est}}$ is at the level of the Heisenberg limit, $\mathcal{L}$ should roughly be independent of N, which can be achieved if $\bar{\ell} \ll N$.

For convenience, we define the reduced Fisher information

$$\mathcal{F} \equiv \frac{F}{4N^2} = \sum_{\ell=0}^{\bar{\ell}} p_{N-\ell}\left(1 - \frac{\ell}{N}\right)^2 \leqslant 1. \qquad (27)$$

Since $\mathcal{L}^2 \leqslant \mathcal{F}$, using Eq. (26), we find

$$\delta^2 \theta'_{\mathrm{est}} \geqslant \frac{1}{4\nu N^2 \mathcal{F}} = \frac{1}{\nu F}, \qquad (28)$$

which indicates that $\hat{\mathcal{O}}$ is generally not an optimal measurement.

It should be noted that the estimator θ'_{est} is biased because of the approximation adopted in Eq. (22). Taking into account the bias, the Cramér-Rao bound for the biased estimator is [57]

$$\langle (\theta'_{\mathrm{est}} - \theta)^2 \rangle_{\mathrm{av}} = \delta^2 \theta'_{\mathrm{est}} + b^2, \qquad (29)$$

where the bias b is defined by $b^2 = \langle (\langle \theta'_{\mathrm{est}} \rangle_{\mathrm{av}} - \theta)^2 \rangle_{\mathrm{av}}$. It can be shown that b is bound by

$$|b| < (2N\mathcal{L})^{-1} \frac{\bar{\ell}^2 \theta^2}{2|\tan(2N\theta)|}.$$

Combined with our assumption, $\bar{\ell}\theta \ll N\theta < \pi/4$, we immediately see that $|b| \ll 1/(2N\mathcal{L})$. Clearly, when $\delta^2 \theta'_{\mathrm{est}} \gg b^2$, or equivalently $\nu \ll 4\tan^2(2N\theta)/(\bar{\ell}\theta)^4$, the bias is ignorable.

IV. NUMERICAL SIMULATION AND DISCUSSION

As seen from the previous section, the most important stage for the proposed Heisenberg-scaled magnetometer is the state preparation. Here we numerically simulate the process of state preparation by considering a realistic system. Specifically, we consider a condensate of ^{87}Rb atoms trapped in a harmonic potential

$$U(\mathbf{r}) = \frac{1}{2} M \omega_\perp^2 (x^2 + y^2 + \kappa^2 z^2), \qquad (30)$$

where $\omega_\perp$ is radial trap frequency and κ is the trap aspect ratio. To obtain the interaction parameters c'_2 and c'_d, we assume the spatial mode of the condensate is the ground state of the trapping potential, i.e.,

$$\psi(\mathbf{r}) = \left(\frac{\kappa}{\pi^3 a_\perp^6}\right)^{1/4} \exp\left[-\frac{1}{2a_\perp^2}(x^2 + y^2 + \kappa z^2)\right], \qquad (31)$$

where $a_\perp = \sqrt{\hbar/(M\omega_\perp)}$ is the length of the radial harmonic oscillator. It can then be evaluated that [48,51]

$$c'_2 = \frac{c_2}{2(2\pi)^{3/2}} \frac{\kappa^{1/2}}{a_\perp^3}, \quad c'_d = \frac{c_d}{6(2\pi)^{1/2}} \frac{\kappa^{1/2}}{a_\perp^3} \chi(\kappa),$$
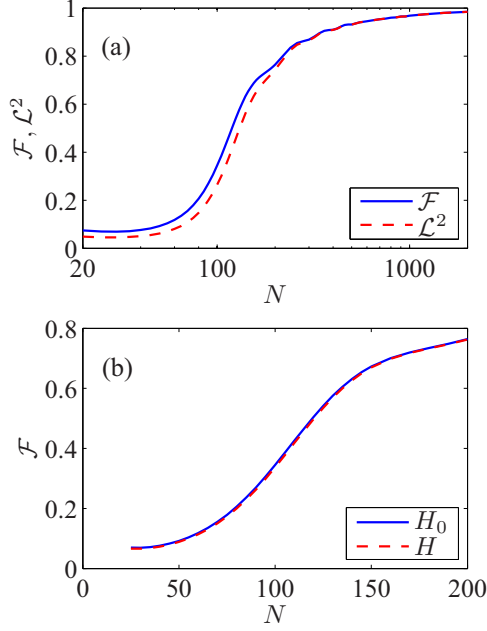
FIG. 3. (a) $\mathcal{F}$ and $\mathcal{L}^2$ as functions of N with the Hamiltonian H_0. (b) Comparison of the reduced Fisher information obtained with Hamiltonian H_0 and H. The sweeping rate is $|v_B| = 10N$.
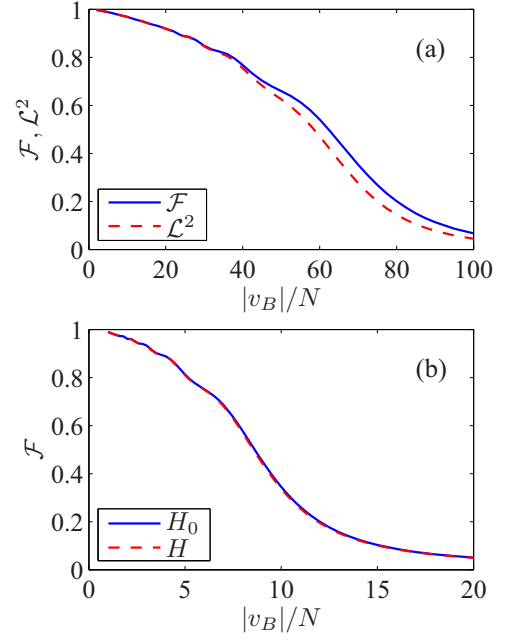

FIG. 4. (a) $\mathcal{F}$ and $\mathcal{L}^2$ as functions of v_B for the Hamiltonian H_0 with $N = 1000$. (b) Comparison of the reduced Fisher information obtained via Hamiltonian H_0 and H with $N = 100$. The sweeping rate v_B is a dimensionless quantity.

where $\chi(\kappa) = (\kappa - 1)^{-1}[2\kappa + 1 - 3\kappa g(\kappa)]$ with $g(\kappa) = \tanh^{-1}\sqrt{1 - \kappa}/\sqrt{1 - \kappa}$. We point out that $\chi(\kappa)$ is a monotonically increasing function of κ, bounded between -1 and 2, and passing through zero at $\kappa = 1$.

For ^{87}Rb atom, we have $g_F = -1/2$, $a_0 = 5.40$ nm, and $a_2 = 5.32$ nm, which leads to $c_2 < 0$ and $c_d \simeq 0.1|c_2|$. To set up the ratio $c = c'_d/|c'_2|$, we take $\kappa = 0.1$ which results in $c \simeq -0.145$. Finally, to fix the unit of time, $\hbar/|c'_2|$, the radial trap frequency is chosen as $\omega_\perp = (2\pi)1000$ Hz such that $\hbar/|c'_2| \simeq 17.4$ s. The numerical simulations are carried out as follows. The initial state $|\Psi_A\rangle$ is taken as the ground state under the magnetic field $B_x = N$, which is larger than the classical saturation field, $-6cN$, and is sufficient to polarize all spins of the condensate. Subsequently, by linearly lowering B_x to zero with a constant sweeping rate v_B, we obtain the wave function $|\Psi_B\rangle$. Typical sweeping rate is chosen such that the total time for the state preparation is achievable in the present-day experiments. Once $|\Psi_B\rangle$ is obtained, it is trivial to find $|\Psi_c\rangle$ and calculate the Fisher information.

In Fig. 3(a), we plot $\mathcal{F}$ and $\mathcal{L}^2$ as functions of N for the Hamiltonian H_0. The sweeping rate is chosen as $|v_B| = 10N$, such that the total time for the state preparation $(0.1\hbar/|c'_2|)$ is independent of N and is reachable in current experiments. Surprisingly, we find that both $\mathcal{F}$ and $\mathcal{L}^2$ approach unit for large N. This behavior can be roughly understood as follows. At the small B_x end of the Hamiltonian H_0, the energy gap between neighboring levels of the lowest few energy levels roughly scale as N. Meanwhile, the sweeping rate v_B is also proportional to N. Consequently, the occupation probability $p_{N-\ell}$ and the highest occupied level $\bar{\ell}$ should roughly remain unchanged for different N. Therefore, according to Eqs. (23) and (27), $\mathcal{F}$ and $\mathcal{L}^2$ approach unit at the large N limit. The result also suggests that the measurement of $\hat{\mathcal{O}}$ approaches

the optimal measurement for sufficiently large N. Figure 3(b) compares the Fisher information of the state $|\Psi_c\rangle$ obtained via the Hamiltonian H_0 and H, respectively. As can be seen, these two curves become visually indistinguishable for $N \gtrsim 100$, indicating that our results obtained with H_0 are applicable to the real system with sufficiently large N.

Next, we explore the sweeping rate dependence of the Fisher information. Figure 4(a) plots $\mathcal{F}$ and $\mathcal{L}^2$ versus the sweeping rate v_B for a state prepared with H_0 containing $N = 1000$ atoms. We find that the reduced Fisher information can be as high as 0.8 even for $|v_B|$ up to $40N$, which indicates that we may significantly reduce the time for state preparation. Moreover, the comparison of the $\mathcal{F}(v_B)$ for the states prepared with H_0 and H in Fig. 4(b) further confirms that the full Hamiltonian H can be well approximated by H_0.

In practice, it is inevitable to have stray magnetic fields that break the parity symmetry and thus lead to initial states significantly deviated from the maximally entangled state. Fortunately, as shall be shown, the Zeeman effect of the stray fields can be eliminated via the dynamical decoupling techniques [54,58]. To see this, we redecompose the Hamiltonian (3) into

$$H = H_x + \delta H,$$
$$H_x = (-1 - c)\hat{\mathbf{S}}^2 + 3c\left(\hat{S}_z^2 + \hat{n}_0\right) - B_x \hat{S}_x,$$
$$\delta H = -\delta\mathbf{B} \cdot \hat{\mathbf{S}},$$

where H_x represents the Hamiltonian required for the initial state preparation and δH is the Zeeman term due the stray field $\delta\mathbf{B}$ which is perpendicular to the x axis. For dynamical decoupling, we apply a sequence of π_x pulses, $\mathcal{D}_x(\pi) = e^{-i\pi\hat{S}_x}$, which rotates the spin of the condensate by π along
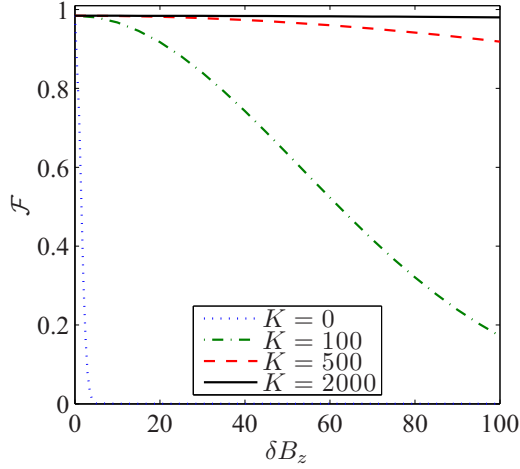
FIG. 5. $\mathcal{F}$ vs δB_z for various pulse numbers. Other parameters are $N = 2000$ and $|v_B| = 10N$. Here δB_z is a dimensionless quantity and, for simplicity, the system is evolved with the Hamiltonian H_0.

the x axis. It can be easily verified that $\mathcal{D}_x^\dagger(\pi) H_x \mathcal{D}_x(\pi) = H_x$ and $\mathcal{D}_x^\dagger(\pi)\delta H \mathcal{D}_x(\pi) = -\delta H$. Now, assuming that the π_x is an instantaneous pulse and the time interval between two adjacent pulses is τ, the time evolution operator after two pulses is

$$U(t = 2\tau) = U_0(\tau)\mathcal{D}_x(\pi)U_0(\tau)\mathcal{D}_x(\pi), \qquad (32)$$

where $U_0(\tau) = e^{-i\tau H} \approx e^{-i\tau H_x} e^{-i\tau \delta H}$ for small τ (i.e., $||H||\tau \ll 1$). By noting that $\mathcal{D}_x^\dagger(\pi) = \mathcal{D}_x(\pi)$, it can be shown that $U(2\tau) \approx e^{-i2\tau H_x}$. Straightforwardly, after periodically applying $2K$ pulses, the evolution operator becomes

$$U(t = 2K\tau) \approx e^{-itH_x} \qquad (33)$$

to the leading order of τ. The effect of the stray field is clearly removed.

In Fig. 5, we plot the Fisher information as a function of the stray field for different pulse numbers. For simplicity, we have neglected the $\hat{n}_0$ term in the Hamiltonian such that we may simulate a condensate with $N = 2000$ atoms. Without loss generality, we assume that the stray field is along the z axis. As can be seen, for $K = 0$, the Fisher information quickly drops to zero even for a very weak stray field. However, the π_x pulse sequence dramatically changes the situation such that the effect of the stray field becomes negligible for $K = 2000$.

Finally, an important issue regarding the initial state preparation is that highly entangled states are fragile against atom losses [59,60]. Consequently, Heisenberg-scaled precision may become unattainable with our configuration. A strict discussion on how atom losses in our system change the precision of the measurement requires a quantitative study which is out of the scope of the present work. Here, we remark that three-body loss can be suppressed by using dynamical decoupling technique [61] or Zeno effect [62]. In addition, a recent theoretical study shows that moderately entangled spin cat states are more robust against particle losses and the measurement precision achievable with these states can still outperform the standard quantum limit [63]. With our system, spin cat states can be easily prepared if the transverse field B_x is not reduced to zero in state preparation [48]. Based on

these discussions, quantum enhanced magnetometer of dipolar spinor condensates may seem plausible.

V. CONCLUSION

To conclude, we have proposed a Heisenberg-scaled magnetometer using spin-1 Rb condensates. Our scheme is based on a protocol which generates the maximally entangled spin state by adiabatically sweeping the transverse magnetic field. We show that the Hamiltonian in the state preparation stage conserves the parity symmetry of the system which significantly shorten the time required for preparing the initial state. We have also proposed a parity measurement scheme using a Stern-Gerlach apparatus, which approaches the optimal measurement in the large N limit. Finally, we show that the phase estimation sensitivity roughly scales with $1/N$.

APPENDIX : CONSTRUCTION OF EVEN- AND ODD-PARITY STATES

Here we construct the explicit form of the parity operator $\hat{\mathcal{P}}$ and determine the parity of the state $|S,m\rangle_x$. To this end, let us first consider the state in the $|S,m\rangle_z$ representation. As shown in Ref. [64], a basis state can be expressed as

$$|S,m\rangle_z = Z_{S,m}^{-1/2}(\hat{A}^\dagger)^{(N-S)/2}(\hat{S}_-)^{S-m}(\hat{a}_1^\dagger)^S|0\rangle, \qquad (A1)$$

where $Z_{S,m}$ is the normalization constant, $\hat{A}^\dagger \equiv [(\hat{a}_0^\dagger)^2 - 2\hat{a}_1^\dagger \hat{a}_{-1}^\dagger]/\sqrt{3}$ creates a pair of atoms in the singlet state, $\hat{S}_\pm \equiv (\hat{S}_x \pm i\hat{S}_y)/\sqrt{2}$, and $|0\rangle$ is the vacuum state. Using Eq. (8), it can be easily verified that $\hat{\mathcal{P}}\hat{A}^\dagger\hat{\mathcal{P}} = \hat{A}^\dagger$ and $\hat{\mathcal{P}}\hat{S}_+\hat{\mathcal{P}} = \hat{S}_-$, from which we derive

$$\hat{\mathcal{P}}|S,m\rangle_z = Z_{S,m}^{-1/2}(\hat{A}^\dagger)^{(N-S)/2}(\hat{S}_+)^{S-m}(\hat{a}_{-1}^\dagger)^S|0\rangle. \qquad (A2)$$

On the other hand, we note that

$$|S,-m\rangle_z = e^{i\vartheta}\mathcal{D}_y(\pi)|S,m\rangle_z, \qquad (A3)$$

where $\mathcal{D}_y(\pi) = e^{-i\pi\hat{S}_y}$ is the rotation operator and ϑ is an arbitrary phase. Utilizing $\mathcal{D}_y(\pi)\hat{a}_{\pm 1}\mathcal{D}_y^\dagger(\pi) = \hat{a}_{\mp 1}$ and $\mathcal{D}_y(\pi)\hat{a}_0\mathcal{D}_y^\dagger(\pi) = -\hat{a}_0$, it can be shown that

$$|S,-m\rangle_z = e^{i\vartheta}(-1)^{S-m}Z_{S,m}^{-1/2}(\hat{A}^\dagger)^{(N-S)/2}$$
$$\times(\hat{S}_+)^{S-m}(\hat{a}_{-1}^\dagger)^S|0\rangle. \qquad (A4)$$

Adopting the Condon-Shortley-Wigner phase convention, $\vartheta + (S-m)\pi = 0$, we obtain

$$\hat{\mathcal{P}}|S,m\rangle_z = |S,-m\rangle_z \qquad (A5)$$

by comparing Eqs. (A2) and (A4), which immediately leads to Eq. (11). Next, to determine the parity of the state

$|S,m\rangle_x$, we note that

$$|S,m\rangle_x = \mathcal{D}_y(\pi/2)|S,m\rangle_z = \sum_{m'} d_{m'm}^{(S)}(\pi/2)|S,m'\rangle_z, \tag{A6}$$

where $d_{m'm}^{(S)}(\pi/2) = {}_z\langle S,m'|\mathcal{D}_y(\pi/2)|S,m\rangle_z$, which satisfies the relation $d_{m'm}^{(S)}(\pi/2) = (-1)^{S-m}d_{-m'm}^{(S)}(\pi/2)$. Now, by $\hat{\mathcal{P}}$ acting on $|S,m\rangle_x$, we find

$$\hat{\mathcal{P}}|S,m\rangle_x = \sum_{m'} d_{m'm}^{(S)}(\pi/2)\hat{\mathcal{P}}|S,m'\rangle_z = \sum_{m'} d_{m'm}^{(S)}(\pi/2)|S,-m'\rangle_z = (-1)^{S-m}|S,m\rangle_x. \tag{A7}$$

Since $N-S$ is always an even integer, the parity of $|S,m\rangle_x$ is even (odd) if $N-m$ is even (odd). Finally, in the $|S,m\rangle_x$ representation, the parity operator can be expressed as

$$\hat{\mathcal{P}} = \sum_{S,m}(-1)^{N-m}|S,m\rangle_{xx}\langle S,m|. \tag{A8}$$

[1] S. A. Murthy, D. J. Krause, Z. L. Li, and L. R. Hunter, Phys. Rev. Lett. **63**, 965 (1989).

[2] C. Chin, V. Leiber, V. Vuletić, A. J. Kerman, and S. Chu, Phys. Rev. A **63**, 033401 (2001).

[3] C. J. Berglund, L. R. Hunter, D. J. Krause, E. O. Prigge, M. S. Ronfeldt, and S. K. Lamoreaux, Phys. Rev. Lett. **75**, 1879 (1995).

[4] G. M. Harry, I. Jin, H. J. Paik, T. R. Stevenson, and F. C. Wellstood, Appl. Phys. Lett. **76**, 1446 (2000).

[5] M. S. Grinolds, P. Maletinsky, S. Hong, M. D. Lukin, R. L. Walsworth, and A. Yacoby, Nat. Phys. **7**, 687 (2011).

[6] Ya. S. Greenberg, Rev. Mod. Phys. **70**, 175 (1993).

[7] I. M. Savukov and M. V. Romalis, Phys. Rev. Lett. **94**, 123001 (2005).

[8] R. Jiménez-Martínez, D. J. Kennedy, M. Rosenbluh, E. A. Donley, S. Knappe, S. J. Seltzer, H. L. Ring, V. S. Bajaj, and J. Kitching, Nat. Commun. **5**, 3908 (2014).

[9] M. Hamalainen, R. Hari, R. J. Ilmoniemi, J. Knuutila, and O. V. Lounasmaa, Rev. Mod. Phys. **65**, 413 (1993).

[10] K. Kobayashi and Y. Uchikawa, IEEE Trans. Magn. **39**, 3378 (2003).

[11] A. Edelstein, J. Phys.: Condens. Matter **19**, 165217 (2007).

[12] V. Giovannetti, S. Lloyd, and L. Maccone, Science **306**, 1330 (2004).

[13] V. Giovannetti, S. Lloyd, and L. Maccone, Phys. Rev. Lett. **96**, 010401 (2006).

[14] V. Giovannetti, S. Lloyd, and L. Maccone, Nat. Photon. **5**, 222 (2011).

[15] D. Leibfried, M. D. Barrett, T. Schaetz, J. Britton, J. Chiaverini, W. M. Itano, J. D. Jost, C. Langer, and D. J. Wineland, Science **304**, 1476 (2004).

[16] M. W. Mitchell, J. S. Lundeen, and A. M. Steinberg, Nature (London) **429**, 161 (2004).

[17] H. Vahlbruch, M. Mehmet, S. Chelkowski, B. Hage, A. Franzen, N. Lastzka, S. Goßler, K. Danzmann, and R. Schnabel, Phys. Rev. Lett. **100**, 033602 (2008).

[18] I. Afek, O. Ambar, and Y. Silberberg, Science **328**, 879 (2010).

[19] B. Yurke, S. L. McCall, and J. R. Klauder, Phys. Rev. A **33**, 4033 (1986).

[20] M. J. Holland and K. Burnett, Phys. Rev. Lett. **71**, 1355 (1993).

[21] Z. Y. Ou, Phys. Rev. A **55**, 2598 (1997).

[22] H. Lee, P. Kok, and J. P. Dowling, J. Mod. Opt. **49**, 2325 (2002).

[23] A. N. Boto, P. Kok, D. S. Abrams, S. L. Braunstein, C. P. Williams, and J. P. Dowling, Phys. Rev. Lett. **85**, 2733 (2000).

[24] J. J. Bollinger, W. M. Itano, D. J. Wineland, and D. J. Heinzen, Phys. Rev. A **54**, R4649 (1996).

[25] D. J. Wineland, J. J. Bollinger, W. M. Itano, F. L. Moore, and D. J. Heinzen, Phys. Rev. A **46**, R6797 (1992).

[26] J. Ma, X. Wang, C. P. Sun, and F. Nori, Phys. Rep. **509**, 89 (2011).

[27] J. A. Dunningham, K. Burnett, and S. M. Barnett, Phys. Rev. Lett. **89**, 150401 (2002).

[28] R. A. Campos, C. C. Gerry, and A. Benmoussa, Phys. Rev. A **68**, 023810 (2003).

[29] C. C. Gerry and J. Mimih, Phys. Rev. A **82**, 013831 (2010).

[30] B. C. Sanders, Phys. Rev. A **45**, 6811 (1992).

[31] B. C. Sanders, J. Phys. A: Math. Theor. **45**, 244002 (2012).

[32] J. Joo, W. J. Munro, and T. P. Spiller, Phys. Rev. Lett. **107**, 083601 (2011).

[33] M. Auzinsh, D. Budker, D. F. Kimball, S. M. Rochester, J. E. Stalnaker, A. O. Sushkov, and V. V. Yashchuk, Phys. Rev. Lett. **93**, 173002 (2004).

[34] I. K. Kominis, Phys. Rev. Lett. **100**, 073002 (2008).

[35] F. Wolfgramm, A. Ceré, F. A. Beduini, A. Predojević, M. Koschorreck, and M. W. Mitchell, Phys. Rev. Lett. **105**, 053601 (2010).

[36] W. Wasilewski, K. Jensen, H. Krauter, J. J. Renema, M. V. Balabas, and E. S. Polzik, Phys. Rev. Lett. **104**, 133601 (2010).

[37] J. M. Geremia, J. K. Stockton, A. C. Doherty, and H. Mabuchi, Phys. Rev. Lett. **91**, 250801 (2003).

[38] J. G. Bohnet, K. C. Cox, M. A. Norcia, J. M. Weiner, Z. Chen, and J. K. Thompson, Nat. Photon. **8**, 731 (2014).

[39] T. Horrom, R. Singh, J. P. Dowling, and E. E. Mikhailov, Phys. Rev. A **86**, 023803 (2012).

[40] W. Muessel, H. Strobel, D. Linnemann, D. B. Hume, and M. K. Oberthaler, Phys. Rev. Lett. **113**, 103004 (2014).

[41] R. J. Sewell, M. Koschorreck, M. Napolitano, B. Dubost, N. Behbood, and M. W. Mitchell, Phys. Rev. Lett. **109**, 253605 (2012).

[42] M. Koschorreck, M. Napolitano, B. Dubost, and M. W. Mitchell, Phys. Rev. Lett. **104**, 093602 (2010).

[43] J. M. Geremia, J. K. Stockton, and H. Mabuchi, Phys. Rev. Lett. **94**, 203002 (2005).

[44] H. T. Ng, Phys. Rev. A **87**, 043602 (2013).

[45] I. Urizar-Lanz, P. Hyllus, I. L. Egusquiza, M. W. Mitchell, and G. Tóth, Phys. Rev. A **88**, 013626 (2013).

[46] H. T. Ng and K. Kim, Opt. Commun. **331**, 353 (2014).

[47] Y.-L. Zhang, H. Wang, L. Jing, L.-Z. Mu, and H. Fan, Sci. Rep. **4**, 7390 (2014).

[48] S. Yi and H. Pu, Phys. Rev. A **73**, 023602 (2006).

[49] M. Vengalattore, J. M. Higbie, S. R. Leslie, J. Guzman, L. E. Sadler, and D. M. Stamper-Kurn, Phys. Rev. Lett. **98**, 200801 (2007).

[50] Y. Eto, H. Ikeda, H. Suzuki, S. Hasegawa, Y. Tomiyama, S. Sekine, M. Sadgrove, and T. Hirano, Phys. Rev. A **88**, 031602 (2013).

[51] S. Yi, L. You, and H. Pu, Phys. Rev. Lett. **93**, 040403 (2004).

[52] S. Yi and H. Pu, Phys. Rev. Lett. **97**, 020401 (2006).

[53] B.-Y. Ning, S. Yi, J. Zhuang, J. Q. You, and W. Zhang, Phys. Rev. A **85**, 053646 (2012).

[54] W. Zhang, S. Yi, M. S. Chapman, and J. Q. You, Phys. Rev. A **92**, 023615 (2015).

[55] C. K. Law, H. Pu, and N. P. Bigelow, Phys. Rev. Lett. **81**, 5257 (1998).

[56] C. Lee, Phys. Rev. Lett. **97**, 150402 (2006).

[57] S. L. Braunstein and C. M. Caves, Phys. Rev. Lett. **72**, 3439 (1994).

[58] C. P. Slichter, *Principles of Magnetic Resonance* (Springer-Verlag, New York, 1992).

[59] R. Demkowicz-Dobrzański, J. Kołodyński, and M. Guţă, Nat. Commun. **3**, 1063 (2012).

[60] Y. M. Zhang, X. W. Li, W. Yang, and G. R. Jin, Phys. Rev. A **88**, 043832 (2013).

[61] C. P. Search, W. Zhang, and P. Meystre, Phys. Rev. Lett. **92**, 140401 (2004).

[62] R. Schützhold and G. Gnanapragasam, Phys. Rev. A **82**, 022120 (2010).

[63] J. Huang, X. Qin, H. Zhong, Y. Ke, and C. Lee, Sci. Rep. **5**, 17894 (2015).

[64] M. Koashi and M. Ueda, Phys. Rev. Lett. **84**, 1066 (2000).